ELSEVIER

Polymer 43 (2002) 2425–2434

polymer

www.elsevier.com/locate/polymer

Co-continuous polycarbonate/ABS blends

J.P.F. Inberg[1], R.J. Gaymans*

Laboratory of Polymer Technology, Department of Chemical Technology, Faculty of Chemical Technology, University of Twente, P.O. Box 217, 7500 AE Enschede, The Netherlands

Received 3 May 2001; received in revised form 22 November 2001; accepted 7 December 2001

Abstract

Co-continuous PC/ABS (50/50) blends were studied with a variable polybutadiene (PB) content (0–40%) in ABS. Polycarbonate (PC), styrene-acrylonitrile (SAN) and PB were blended in two steps using a twin screw extruder. Rectangular bars were injection moulded and notched Izod impact tested at different temperatures and in single edge notch tensile tests at 1 m/s and different temperatures. Co-continuous PC/ABS gave a brittle-to-ductile transition temperature lower than expected based on notched Izod results for dispersed ABS in PC. The brittle-to-ductile transition temperature, in the co-continuous PC/ABS blends, decreased with increasing rubber content in SAN. The fracture energies showed an optimum at 15% PB in SAN while at the same time a delamination was seen on the ductile fracture surface, due to failure of the PC/SAN interface. Delamination disappeared when the rubber content in SAN or the temperature was increased. Specimens containing a welding were injection moulded to study the influence of rubber and AN content in the SAN on the interface. Weldline strength of the blends was very poor compared to PC, but improved with increasing rubber content in SAN. © 2002 Elsevier Science Ltd. All rights reserved.

Keywords: Polycarbonate; Co-continuous blends; Weldline

1. Introduction

In the mixing of two immiscible polymers, a two phase structure is formed. Beside processing dependent factors like applied shear, the morphology is strongly dependent on volume and viscosity ratio and the magnitude of interfacial tension between the components [1–3]. The component that occupies most space will most likely assume the role of continuous phase. However, the component with lower viscosity will tend to encapsulate the more viscous component, since this reduces the rate of energy dissipation by mixing. Thus regions in viscosity-composition space may occur, where either component A or B will be the continuous phase, as shown in Fig. 1.

A transition zone exists where both A and B will not form the dispersed phase, so both components can form continuous phases simultaneously. Such an interpenetrating network can be generated in many systems. In such morphology, the two immiscible phases each remain connected throughout the blend. So each component contributes to the load bearing and this reduces somewhat the need for transferring the stress across a phase boundary [2]. Therefore, the interphase adhesion in co-continuous blends is not as critical for good mechanical properties. Immiscible blends with interpenetrating phases show improved mechanical properties relative to the usual dispersed/continuous phase systems [2]. Mamat et al. [4] studied a nylon-6/ABS blend over the entire composition range and found a peak for elongation at break and impact properties around 70% ABS content. A co-continuous morphology was observed at this composition. The peak in the results was attributed to this morphology.

Lee et al. [5] extensively studied the morphology of a PC/ABS blend throughout the entire composition range. The PC-rich blends showed dispersed ABS in a bead-and-string structure. With increasing ABS content, the bead-and-string structures became more densely arrayed and more interconnected. A morphology transition was observed between the 70/30 and 60/40 compositions, from the bead-and-string structure to a coalesced structure. For the 40/60 compositions, PC formed a dispersed phase with styrene-acrylonitrile (SAN) inclusions. The ABS-rich blends showed PC domains dispersed in the continuous ABS phase. Differences in morphology were observed at different locations in the injection moulded specimens. However, properties of these blends were not reported.

Many researchers have reported on PC/ABS blends and their behaviour. Most of the research considers dispersed

* Corresponding author.
E-mail address: r.j.gaymans@ct.utwente.nl (R.J. Gaymans).
[1] Currently at Wavin, Dedemsvaart, The Netherlands.

PII: S0032-3861(01)00813-8

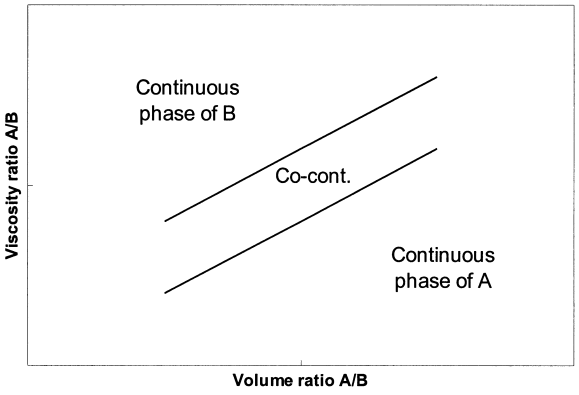

Fig. 1. Effect of relative component proportion and viscosity on phase morphology [2].

ABS and the co-continuous morphologies are investigated much less [5,6]. This is peculiar, since many industrial PC/ABS blends have a co-continuous structure. No extensive study on the properties of a co-continuous PC/ABS blend was found in open literature. The research aim of this paper, therefore, is to look at co-continuous PC/ABS blends and study the influence of rubber concentration in the ABS phase on the notched impact behaviour.

2. Experimental

2.1. Materials

Commercially available PC, SAN and SAN/PB were kindly supplied by GE Plastics and DOW Benelux. The materials are specified in Table 1. PC/ABS (50/50) blends were made to study the behaviour of a co-continuous PC/ABS blend.

Polycarbonate has a notched Izod impact value of about 10 kJ/m^2 at room temperature, and of about 55 kJ/m^2 at 50 °C. Pure SAN fractures at impact values below 5 kJ/m^2, up to high temperatures [7]. The SAN Tyril 790 was chosen to match the melt flow rate of the PC as closely as possible.

Table 1
Material properties

Trade name	Provided by	Description
PC: Lexan™ HF1110R	GE Plastics	Bisphenol A polycarbonate, density 1.20 g/cm^3 MFR = 25 g/10 min
SAN: Tyril™ 790	DOW Benelux	Styrene-acrylonitrile, 29% AN density 1.08 g/cm^3 MFR = 21 g/10 min
PB: GRC™ 310	DOW Benelux	ABS: SAN grafted PB powder PB content 50%, particle size 0.1 μm

2.2. Specimen preparation

Compounding of the materials was done in two steps using a Berstorff (ZE 25 × 33D) twin screw extruder. In the first extrusion step at barrel zone temperatures 185/190/190/190/200/200/200 °C and screw speed 200 rpm, SAN was mixed with different amounts of a core shell rubber (Polybutadiene/SAN) rubber, producing ABS with various wt% PB. PB content in ABS was varied between 0 and 40%. In the second extrusion step at barrel zone temperatures of 215/220/220/220/230/230/230 °C and 200 rpm, the SAN/PB was blended into PC, producing a PC/ABS (50/50) blend.

After compounding, the blends were injection moulded into rectangular bars of 74 × 10 × 4 mm^3, using an Arburg Allrounder 221-55-250 injection moulding machine. Moulding temperature was 230 °C, mould temperature 80 °C and injection pressure 55 bar at 100 rpm screw speed.

A single-edge V-shaped notch of 2 mm depth and tip radius 0.25 mm was milled in the specimens.

2.3. SEM photography

Scanning electron microscopy pictures were taken to study the morphology of the different blends. Specimens were taken from the core of the injection moulded bars. SEM specimens were prepared by cutting with a CryoNova microtome at 110 °C with a diamond knife (−100 °C) and cutting speed of 0.2 mm/s. The cut surfaces were then sputter-coated with a thin gold layer and studied with a Hitachi S-800 field emission SEM.

2.4. TEM photography

TEM microscopy study was performed at DOW Benelux. The specimens were embedded in Epofix epoxy resin and cured for 24 h at room temperature. The specimens were cross-sectioned with a diamond Histo knife until the middle of the specimen was reached. The specimens were initially trimmed with a Leica ULTRACUT E ultramicrotome at room temperature using a diamond-trimming knife, then stained overnight with OsO_4 vapour and finally ultra-thin sectioned with a Leica ULTRACUT E ultramicrotome using a diamond knife. The section thickness was 70 nm. The ultra-thin sections were placed on a 400-mesh carbon-coated copper grid and studied with a Philips CM12 transmission electron microscope operating at 120 kV. TEM micrographs were made of the area around an arrested crack in the specimens, at 11200 and 2100 × magnifications.

2.5. Notched Izod impact tests

Notched Izod impact tests were carried out using a Zwick pendulum machine equipped with a 40 kpcm hammer. In order to determine the brittle-to-ductile transition temperature, the specimens were tested at different temperatures, by

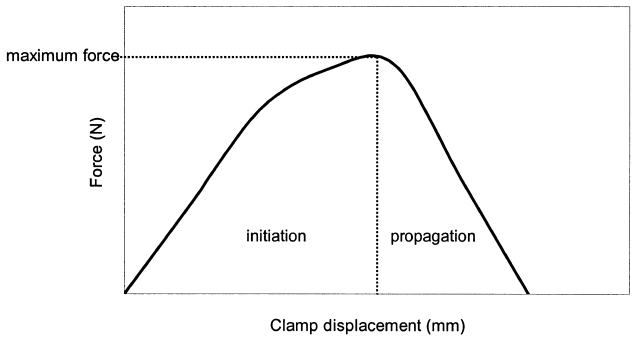

Fig. 2. Schematic representation of a force–displacement curve obtained from a SENT test.

placing them in a Lauda thermostatic bath prior to testing. All measurements were performed in five-fold.

2.6. Single edge notch tensile tests

Notched specimens (rectangular bars of $74 \times 10 \times 4$ mm^3) were fractured at different temperatures in single edge notch tensile (SENT) tests. A Schenck VHS servohydraulic tensile test machine was used with a clamp speed of 1 m/s. All measurements were performed in five-fold.

The specimen length between the clamps is 35 mm, resulting in a macroscopic strain rate of 28.5 s^{-1}. The piston has a pick-up unit with damped contact to allow fast acceleration of the pick-up arm and specimen without severe oscillations. Clamp displacement is assumed to equal the piston displacement. A piezo force transducer is located between the crosshead and the upper clamp. Force, time and displacement signals are registered and stored using an Adamscope transient recorder with a maximum specimen rate of 2 MHz per channel. Force–displacement signals result and allow for energy determination by calculating the area under the force–displacement curve (Fig. 2).

The tensile machine is equipped with a temperature chamber, which enables measurements at temperatures in a range of −100 to +160 °C. The temperature chamber is heated, or cooled with a nitrogen flow, which passes through liquid nitrogen and is subsequently heated to the set temperature.

The fracture process may be divided into two stages. The crack initiation stage starts from zero displacement, and crack initiation is assumed to take place at the point of maximum stress. All displacement after this point of maximum force contributes to crack propagation, which is the second stage of the fracture process. Brittle fracture is characterised by zero propagation displacement.

Parameters used to describe the fracture process are:

- maximum stress: maximum force on the force–displacement curve, divided by the initial cross-sectional area behind the notch (32 mm^2). Stress concentrations behind the notch are neglected
- crack initiation displacement: clamp displacement between the first point of force-rise and the maximum force
- crack initiation energy: area under force–displacement curve up to maximum force
- crack propagation displacement: clamp displacement between the point of maximum force and the first point of zero force after force-fall
- crack propagation energy: area under force–displacement curve after maximum force
- fracture displacement: summation of initiation and propagation displacement
- fracture energy: summation of initiation and propagation energy.

2.7. Infrared thermography

The temperature rise during fracture of specimens containing notches of radius 0.25 mm was monitored using an infrared camera. Specifications are listed in Table 2. Only temperatures at the surface of the specimen can be determined with the infrared camera. Temperatures inside the specimen are expected to be higher than at the surface. The spot size of about 100 μm is relatively large. The temperature indicated in one spot is an average temperature over the spot size. The temperature directly at the fracture surface, which is expected to be highest, therefore cannot be determined.

3. Results and discussion

PC/ABS blends were made both with the ABS dispersed as with the ABS continuous in the PC phase. By increasing the ABS content (with 15 wt% PB in the ABS) we observed a complex change in brittle-to-ductile transition temperatures (Fig. 3). At low ABS contents the brittle-to-ductile transition temperature (T_{bd}) was not lowered (0–20 wt%) while at high ABS contents (50 wt%) the blends had a very low T_{bd}. The transition from dispersed to continuous ABS-phase occurred between 35 and 45% ABS content in PC. The decrease in T_{bd} was thus unexpectedly strong at the transition to co-continuous structure.

The behaviour of the co-continuous PC/ABS (50/50) material was studied in more detail. Extrusion and injection moulding of the materials showed that the materials were easy to process, except for the PC/SAN (50/50) (mixture without rubber). This PC/SAN material was difficult to compound

Table 2
Technical data for the infrared camera, equipped with close-up lens. Data is from manufacturer's data sheet

TVS 600 AVIO Nippon Avionics Co., Ltd	
Temperature range	− 20 to 300 °C
Temperature resolution	0.15 °C
Spectral range	8–14 μm
Image rate	30 frames/s
Spatial resolution	0.1 mm spot size

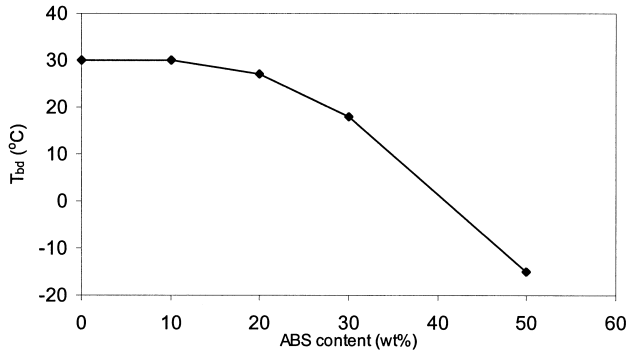

Fig. 3. Brittle–ductile transition temperature of PC/ABS, measured in Izod, as function of ABS content, ABS containing 15% PB.

as the melt exhibited a high elasticity. A small flaw on the extruded thread caused fast rupture of the thread. However, an increase in feeding rate of the extruder solved this problem.

In the discussion later, the material designation is *x*% blend, where *x* represents the weight content PB in the ABS and the PC/ABS ratio is always 50/50.

3.1. Morphology

SEM pictures of the PC/ABS (50/50) blends show a layered co-continuous morphology for all blends. Layer thickness for both phases were about 0.3–2 μm. Rubber content of the ABS did not seem to influence the ABS layer thickness. Orientation was in the injection moulding direction. The GRC rubber was well dispersed in the SAN in all blends, with only a few rubber particle clusters (see Figs. 4 and 5).

3.2. Notched Izod tests

3.2.1. Izod impact values

Co-continuous PC/ABS blends were studied in notched Izod tests as a function of test temperature. The PB content in the ABS phase was varied from 0 to 40%.

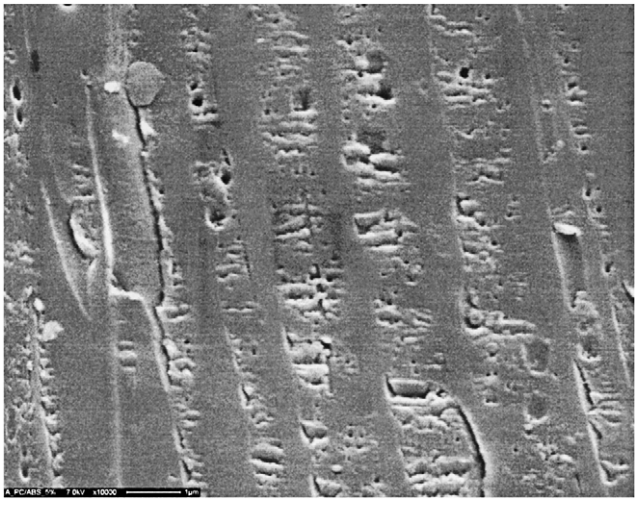

Fig. 4. SEM picture of PC/ABS (50/50), undeformed sample, ABS containing 5 wt% PB (10 × 12 μm).

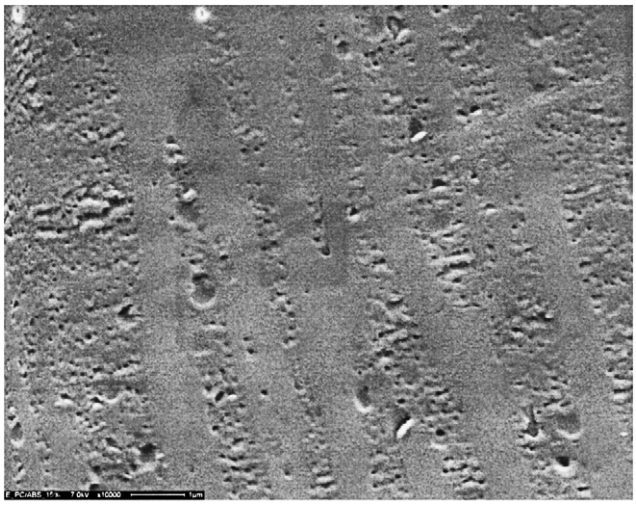

Fig. 5. SEM picture of PC/ABS (50/50), undeformed sample, ABS containing 15 wt% PB (10 × 12 μm).

At low temperatures, the 0 and 5% PB-blends gave very low Izod impact values, but impact values increased gradually with rubber content (Fig. 6). At high temperatures (140 °C), the 0% blend gave tough fracture and impact values approached the tough PC notched Izod value. At 80–140 °C, impact values for the 5% blend were very low; for the blends with PB content in ABS above 5% the impact values were higher and the 10–40% blends appear to reach about the same level.

The intermediate temperature (0–80 °C) showed more distinct differences between the blends. The 0% blend had a constant, low level. The 5, 10 and 15% blend, however, appeared to go through a maximum in impact values. This was especially the case for the 15% blend. The 20, 30 and 40% blend did not show this unusual maximum in Izod values. It was surprising to see that the fracture surface showed delamination and pull-out of material at these peak impact values in the 10 and 15% PB blends (Fig. 7).

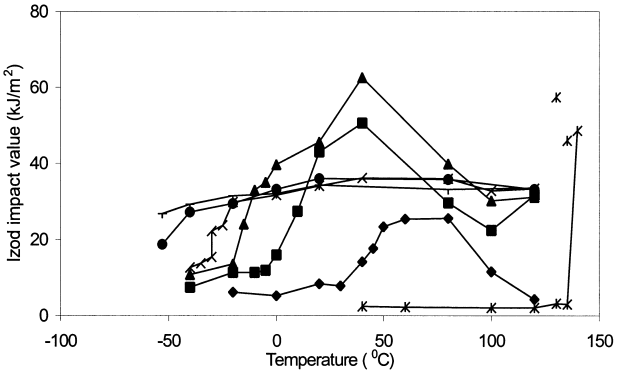

Fig. 6. Notched Izod values for the PC/ABS (50/50) blend with different wt% PB in ABS (∗: 0%, ◆: 5%, ■: 10%, ▲: 15%, ×: 20%, ●: 30%, +: 40%).

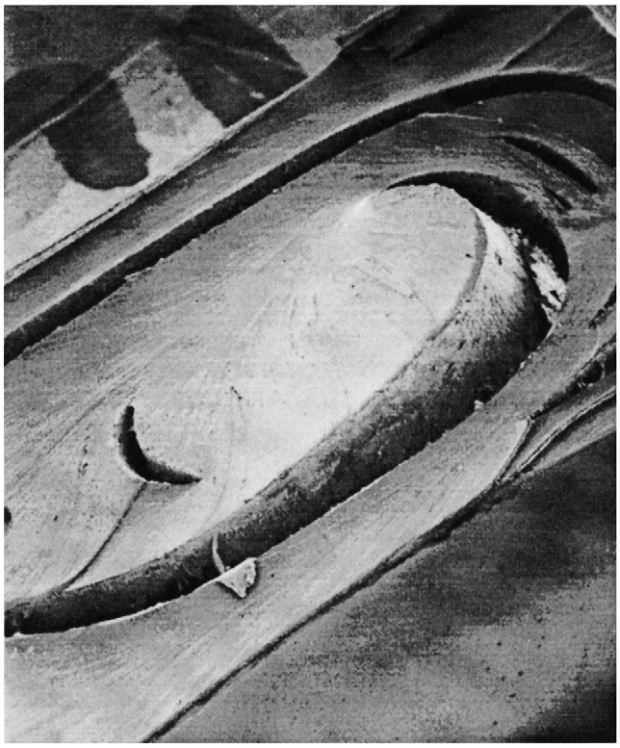

Fig. 7. Fracture surface of a sample (15 wt% PB in ABS, PC/ABS (50/50) blend) fractured at 40 °C with the notched Izod method. Propagation from top right to bottom left, the whole width of the 4 mm sample is shown. A strong delamination in the fracture surface can be seen.

Steenbrink [8] showed that increasing the rubber concentration in SAN/PB blends increased the impact values. However, the brittle-to-ductile transition temperature did not change. From Figs. 6 and 8 it is apparent that, for the PC/ABS material, the addition of rubber did not change only the impact values. The brittle-to-ductile transition temperature changed as well and a delamination region could be observed. The boundaries of this region appeared to be determined by T_g of SAN (110 °C) and the rubber content in ABS. PC/ABS 0% blend (actually a PC/SAN blend) had a brittle-to-ductile transition temperature of 135 °C, which is much higher than the T_{bd} of pure PC. The PC is greatly embrittled by the SAN phase. The transition temperature decreased with increasing rubber content in ABS. This decrease was strongest at low rubber concentrations. At high concentrations very low transition temperatures were achieved.

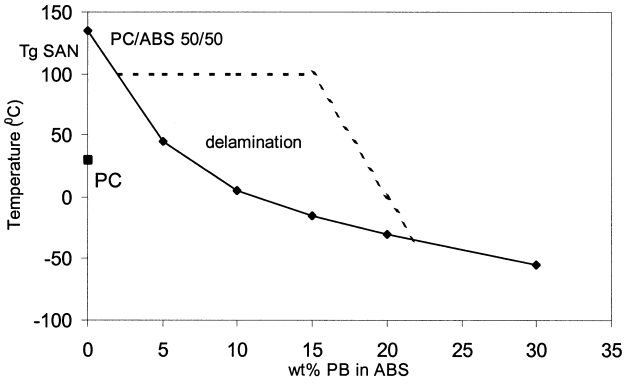

Fig. 8. PC/ABS (50/50) brittle–ductile transition temperatures at different wt% PB in ABS (notched Izod). 40% T_{bd} could not be determined in notched Izod. The area in which delamination was observed is bounded by the lower full curve and the dashed curve.

The impact values as a function of temperature appeared to go through a maximum at higher temperatures, between 20 and 80 °C (Fig. 6). This effect was very strong for the 10 and 15% blends. This would suggest that an optimal rubber content exists in the ductile region. At 40 °C the 15% blend showed the best results (Fig. 9). At low temperatures (−20 °C) more rubber in ABS improved the Izod properties, up to 20% PB. At higher PB concentrations, however, the Izod impact values remained constant. Apparently, in the 20% blend, enough rubber is present to relieve the triaxial stress state in the material and prevent delamination from taking place. The additional rubber is not needed (at −20 °C), and will likely not cavitate, because the plane strain situation is already changed into one of plane stress. Therefore the additional rubber makes no contribution to notched Izod impact values at this temperature.

At the peak values, the fracture surfaces showed delamination and pull-out (Fig. 7). It appears that delamination can cause thin layers of material to be loaded during fracture. These thin layers are more likely to yield and this might give additional energy absorption. This could account for the high impact values, slightly higher than pure PC (about 55 kJ/m^2 at room temperature).

So in the brittle, low temperature region adding rubber increases fracture energies. In the ductile, high temperature region at low rubber concentrations the results include both the effect of rubber content and the contribution of delamination. The rubber is very effective in decreasing T_{bd}.

3.2.2. Fracture surfaces

The surfaces of the fractured specimens were studied. With brittle fracture the surface was smooth and no stress whitening was visible. A white, ductile line appeared just ahead of the notch with increasing temperature. The size

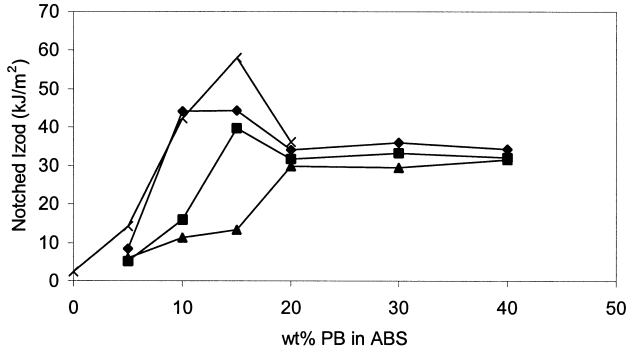

Fig. 9. Izod values at different temperatures (×: 40 °C, ◆: 20 °C, ■: 0 °C, ▲: −20 °C).

increased with increasing ductility of the fracture until the fracture surface was completely ductile. The thickness of the stress whitened zone below the ductile fracture surface was small, the size ranging from about 0.5 mm for the 5% blend to 1.5 mm for the 40% blend.

On the ductile and whitened fracture surface, a macroscopical delamination structure was sometimes visible (Fig. 7). The dark, broad lines in this photo are locations where material has detached. These ruptures go into the material for up to 1 mm in a direction perpendicular to the fracture surface.

A close-up SEM picture of one of these ruptures revealed that the delamination is apparently caused by failure of the PC/ABS interface (Fig. 10). The dark line in the top right of the picture is the tip of a delamination rupture. It seemed that delamination occurred along the PC/ABS interface. Possibly the adhesion between the PC and SAN phase is not optimal. The delamination effect was strongest at low rubber content and disappeared at higher rubber content, above 20 wt% (Fig. 8). The triaxial stresses are reduced at high rubber contents and delamination is less probable. The 0% blend fractured in a brittle manner up to high test temperatures and did not show this delamination structure, having a brittle-to-ductile transition temperature of 140 °C. The structure appeared at the brittle-to-ductile transition temperature and above, and disappeared at temperatures above 100 °C for low rubber content. The surface of the 20% blend was almost completely without delamination at 40 °C. Yield stress decreases at higher temperatures. As a consequence, the plane strain stress situation is not as severe as at lower temperatures. Therefore delamination will not be as extensive under these conditions. At higher rubber contents more rubber particles are available for cavitation, relieving plane strain conditions and thereby preventing delamination. Apparently, a competition exists between rubber cavitation and delamination. The formation of the delamination structure apparently results in formation of additional surface as well as additional deformation of the material. Layers of material, which formed by delamination, yielded during fracture and protrude from the fracture surface. This is visible on both sides of the fractured specimen, indicating additional deformation. Maximal material protrusion out of both fracture surfaces was 2 mm for the 15% blend at 40 °C, at the highest Izod value in Fig. 6.

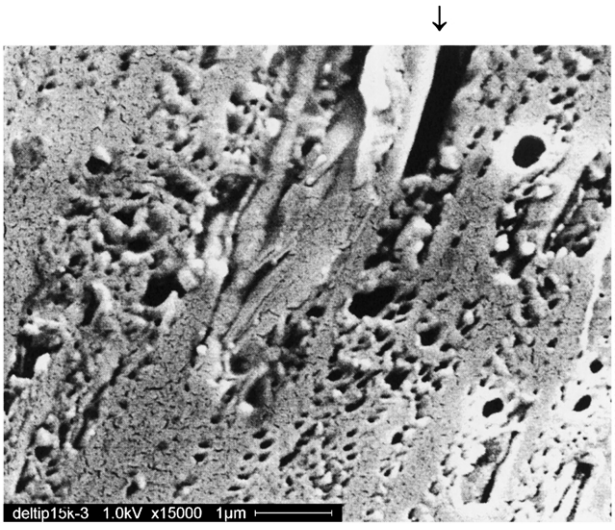

Fig. 10. Delamination in PC/ABS blend (15%, 40 °C), arrow indicates the tip of delamination tear and growth direction, going from fracture surface down into the material.

3.2.3. PC/SAN interface

To measure the adhesion of SAN to PC, tensile tests were done on specimens containing a weldline. These experiments were done for PC, PC/SAN and PC/ABS blends. Two other SAN Tyril types were used in PC, containing 25 and 27% AN, to look at the influence of AN content of the SAN on the weldline strength. The weldline was obtained during injection moulding, by injecting materials from both sides into the mould. This resulted in a standard dumbbell specimen with a weldline in the middle. Tensile testing of these specimens might give an indication of interfacial strength.

From the TEM pictures of the weldline in PC/SAN (50/50), it is clear that the weldline in the material represents a shallow sharp notch (Fig. 11). Assuming that for all tested materials a similar small, sharp notch is present at the specimen surface, this tensile weldline test can measure the delamination stress due to high triaxiality ahead of the notch.

Weldline strengths of PC/SAN were extremely low, indicating that the presence of a weldline results in very poor properties (Fig. 12). Differences between the different AN types were not large. This was quite unexpected since optimal adhesion with PC has been reported at 27% AN content in SAN [9,10]. However, AN content in SAN did not appear to have a significant influence on the weldline strength.

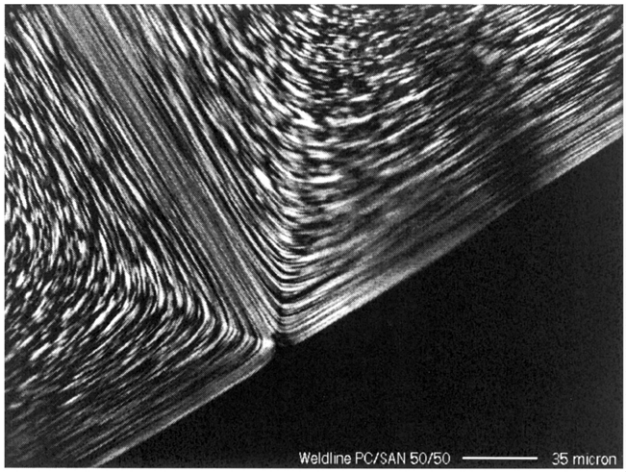

Fig. 11. SEM picture of the weldline morphology of a PC/SAN (50/50) blend.

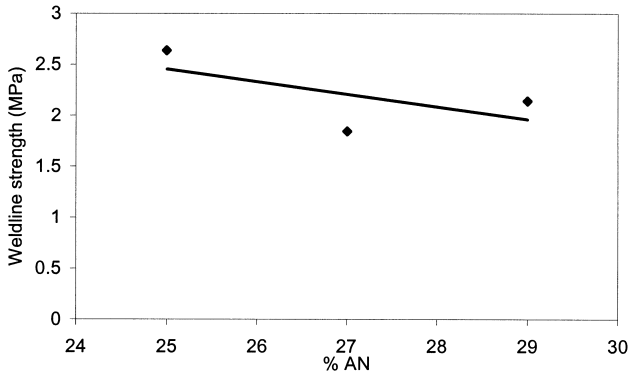

Fig. 12. Influence of AN content in SAN on weldline strength in PC/SAN (50/50) blend.

Pure PC showed much higher weldline strength than the PC/ABS blends (Fig. 13). The weldline strength in PC was close to the yield stress of PC (±60 MPa), and these specimens even showed necking during tensile testing, as occurs in 'normal' specimens.

Pure SAN showed extremely low weldline strength, only somewhat better than PC/SAN. The weldline in the specimen acts as a notch, leading to brittle behaviour of the SAN. This however is in contradiction with the high strength of the notch-sensitive PC. The PC/ABS blends showed a somewhat improved weldline strength compared to PC/SAN, but nowhere near that of the pure PC weldline strength. The rubber does contribute somewhat to the weldline strength, although the weldline still represents a major defect in the material. Possibly the severe triaxial stress state near the weldline is reduced due to rubber cavitation, leading to a higher weldline strength.

3.3. Single edge notch tensile tests

During the SENT test, force and clamp displacement are recorded, and fracture energy can be determined, as Section 2. Co-continuous PC/ABS blends with PB content in ABS ranging from 0 to 40% were tested in SENT at 1 m/s and room temperature to study the effect of the amount of PB in the SAN-phase. The co-continuous PC/ABS blend with ABS containing 15% PB was also studied as a function of temperature.

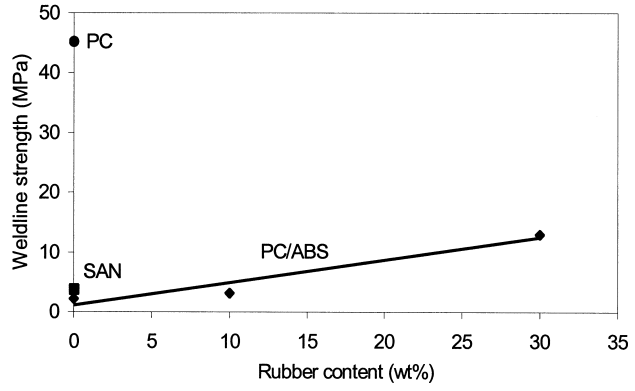

Fig. 13. Influence of ABS rubber content on weldline strength of co-continuous PC/ABS blends (◆), compared with weldline strength in PC (●) and SAN (■).

3.3.1. Influence of PB content in SAN

SENT tests were done at 1 m/s and room temperature for blends containing different wt% PB. PC/SAN without rubber had a very low fracture stress (Fig. 14a). Adding 5% PB in the SAN increased this fracture stress significantly, also changing from brittle-to-ductile fracture. The maximum stress in the ductile region remained constant between 10 and 20% PB, possibly due to delamination. In the ductile region above 20% PB, the maximum stress decreased, due to increasing rubber content.

Fracture displacement increased steadily with PB content, although the effect became much less strong at higher rubber content (Fig. 14b). The transition from

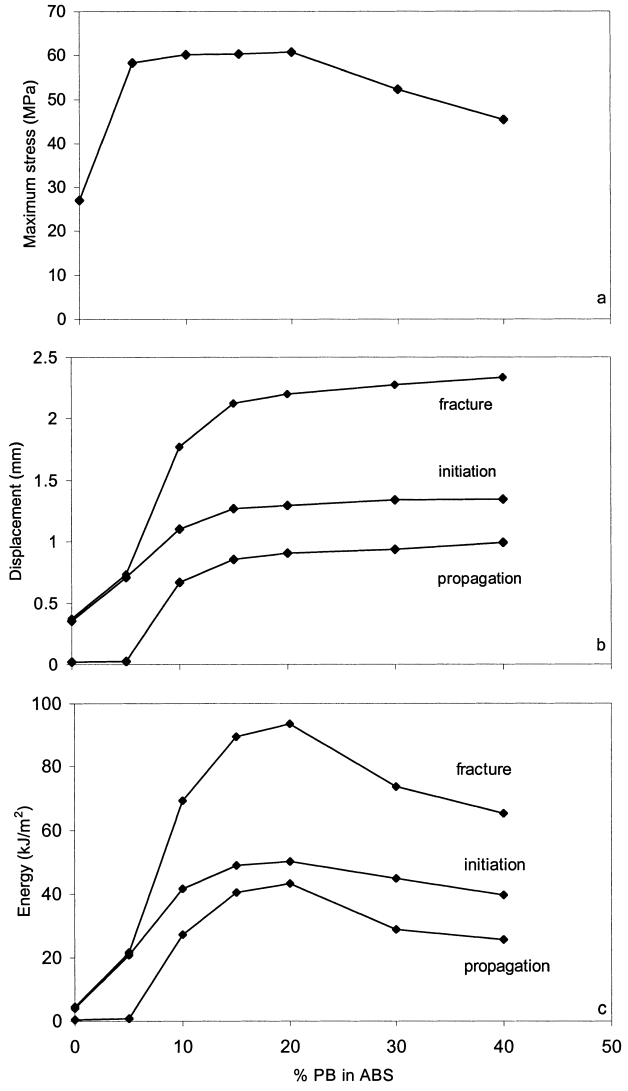

Fig. 14. PC/ABS (50/50) SENT results: influence of PB content in ABS (1 m/s, room temperature).

brittle-to-ductile fracture at 20 °C took place between 0 and 10% PB. For dispersed ABS, a gradual decrease in fracture displacement was seen with higher ABS content.

Fracture displacement results were split into initiation and propagation. Propagation displacement clearly showed the transition from brittle-to-ductile fracture. Adding more rubber gave an increase in both initiation displacement and propagation displacement in the ductile region. At rubber contents of 20% and above, displacement results were hardly influenced by rubber content.

Fracture energy increased with PB content up to 20% PB in ABS (Fig. 14c). The decrease above 20% PB coincided with the decrease in maximum stress. An optimal rubber concentration appeared to exist at room temperature, as was found in the notched Izod experiments.

The previously described delamination structure appeared again on the fracture surfaces, although pull-out of material was less pronounced than in the Izod tests. Brittle fracture showed no delamination marks on the fracture surface. Increasing rubber content resulted in less delamination in the ductile region. No delamination was visible on the ductile fracture surface of the blends with ABS containing 30 and 40 wt% PB, probably because the rubber relieves the plane strain situation enough so that no delamination can take place. Apparently, a competition exists between delamination and rubber cavitation. A PB content of 15% in ABS is apparently not sufficient to prevent delamination. Delamination is prevented at a PB content of 30% and higher.

Infrared camera measurements were done to determine the temperature development during testing. Maximum surface temperature was determined (Fig. 15a). It appeared that an increasing PB content in ABS led to a decrease in maximum temperature. At the same time, the size of the temperature zone changed and became thicker (Fig. 15b). The increase in temperature zone size agrees with the propagation displacement results (Fig. 14b) which also increased with rubber content in ABS. Apparently, the deformation in low rubber-content blends is more localised. Local temperature will therefore reach a higher value.

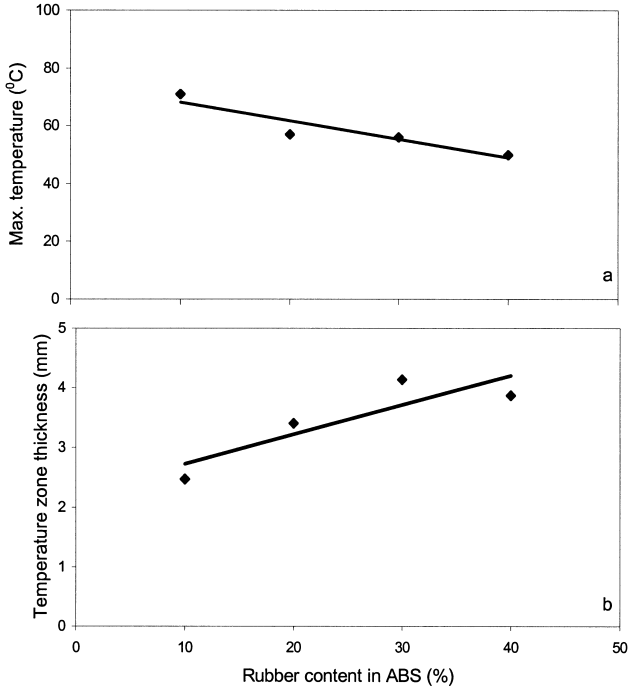

Fig. 15. Influence rubber content in ABS on temperature zone development during SENT tests at 1 m/s and room temperature.

3.3.2. Influence of test temperature

The 15% blend has a T_{bd} of −15 °C in notched Izod. This PC/ABS blend (ABS containing 15% PB) was also tested in SENT tests across the complete temperature range (Fig. 16).

At low test temperatures, the maximum stress was about 55 MPa. At high temperatures, the maximum stress dropped to about 20 MPa, due to decreasing yield stress (Fig. 16a). Fracture displacement increased steadily with temperature, as did propagation displacement. Test temperature had no significant effect on initiation displacement (Fig. 16b). At low temperatures, the fracture energy increased with

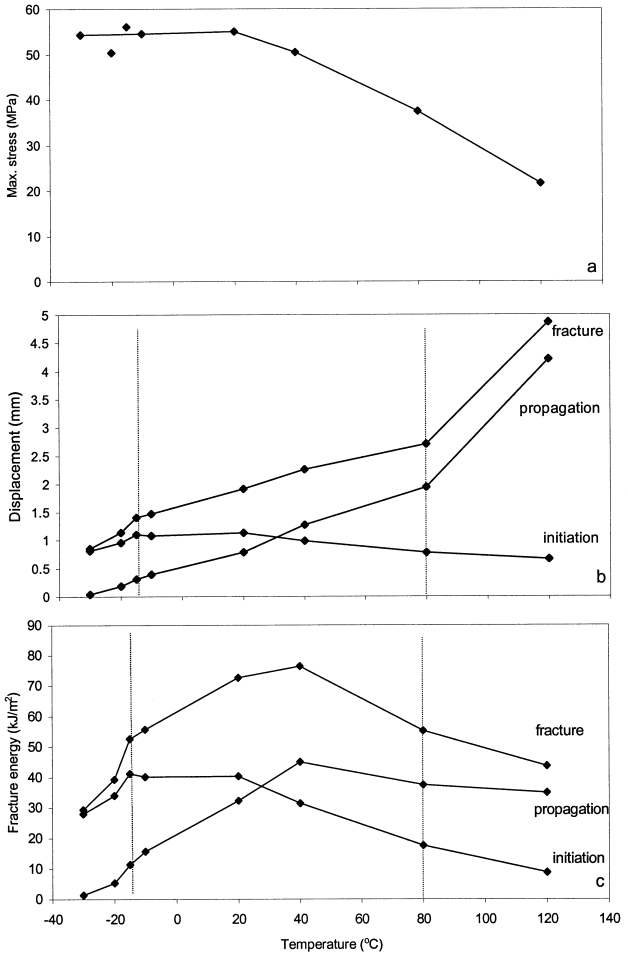

Fig. 16. SENT (1 m/s) results for PC/ABS (50/50) 15% blend at different temperatures. Also indicated the temperature range in which delamination was observed.

temperature (Fig. 16c). At higher temperatures, fracture energy decreased with increasing temperature. Fracture energy appeared to go through a maximum, as did propagation energy. At higher test temperatures, yield stress will decrease, leading to lower energy absorption. At low temperatures, initiation energy increased slightly with temperature, but decreases with increasing temperature in the ductile range.

Based on propagation results and fracture surface appearance, the brittle–ductile transition temperature in SENT was determined as occurring between −20 and −15 °C for the PC/ABS 15% blend. This corresponds to a T_{bd} of −15 °C that was found in notched Izod testing. Delamination was observed on the fracture surfaces between first ductile fracture at −20 °C up to about 80 °C. Pull-out of material was much less pronounced than in the notched Izod tests. Maximum material protrusion out of both surfaces was 0.8 mm, much less than the 2 mm measured for Izod. This difference possibly originates from the different way of loading the material in Izod and SENT tests. In SENT, material is loaded purely in the tensile direction, while Izod involves bending [11]. Comparing notched Izod and SENT energy absorption results, we see that the influence of temperature on the results of these tests is comparable (Fig. 17). This would suggest that the two test methods are also comparable, as was already suggested in literature [12].

TEM pictures were made of an arrested crack in a PC/ABS (50/50) specimen, tested at 1 m/s (Fig. 18). The co-continuous structure is visible, with PB particles in the SAN material. Only few rubber particles were found in the PC phase. Cavitated rubber particles in the SAN-phase appear as white holes in the pictures. Some cavitated particles apparently grew together and formed larger cavities in the SAN. It appeared that the PB particles that have cavitated are located in bands through the material. Crazes in the SAN are visible that initiated from cavitated particles and have grown to the PC/SAN interface. Closer to the crack tip the rubber had less cavities, as was also found by Steenbrink [13]. Deformed rubber particles are also visible in this region, indicating that the SAN phase has deformed and

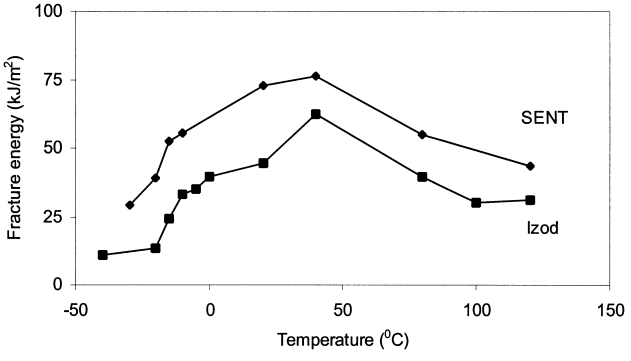

Fig. 17. SENT test fracture energy results (1 m/s), compared to notched Izod results for PC/ABS (50/50) blend, ABS containing 15% PB.

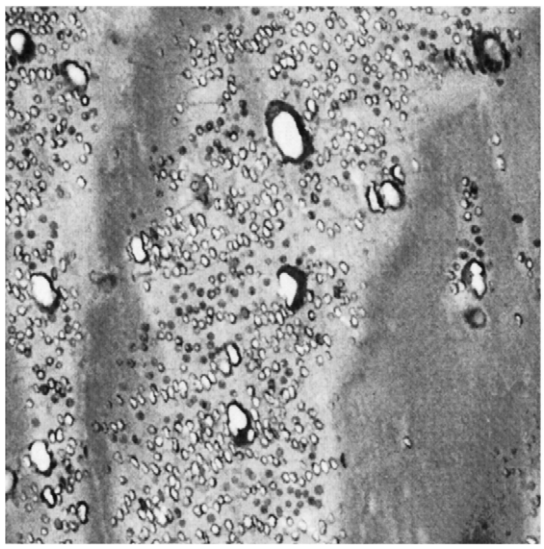

Fig. 18. TEM micrographs of damage zone ahead of an arrested crack in the centre of the specimen tested in SENT at 1 m/s and loaded in the vertical direction. PC/ABS (50/50), ABS containing 15% PB, (8 × 8 μm).

probably also the PC phase. The crazes in the SAN phase sometimes appeared to originate from uncavitated particles. However, this effect was not substantial enough to confirm the hypothesis of Steenbrink [13] that the cavitated rubber particles are closed due to elastic unloading.

It was also observed that in some locations the PC/SAN interface has detached. This is not shown here, but confirms that delamination can occur in the material along the PC/SAN interface at high strains.

In conclusion, upon loading the material, rubber particles in the SAN phase will cavitate. Crazes will form and grow in the SAN-phase, until these crazes reach the PC phase. The PC phase will then yield and eventually the material will fracture.

4. Conclusions

Co-continuous polycarbonate/ABS blends can be obtained by mixing PC and ABS in a 50/50 ratio. The brittle-to-ductile transition temperature, T_{bd}, decreased in notched Izod with increase of the PB rubber content in the ABS. However, in the ductile region, higher rubber content does not necessarily result in higher impact values. It does guarantee ductile behaviour at low temperatures. An optimal rubber content in ABS of about 15% exists in the ductile region. Co-continuous PC/ABS gave a lower T_{bd} than expected, based on notched Izod results for ABS dispersed in PC.

It was found that the SENT tests at 1 m/s are comparable to notched Izod impact tests. The SENT tests confirm the effect of increasing PB content in ABS. An optimal PB content exists in the ductile region.

In both SENT and Izod tests delamination of PC/SAN interface resulted in an observable delamination structure on the fracture surface. An increase in test temperature or rubber content in the ABS diminished this effect. This indicates that a competition exists between rubber cavitation and the delamination process. Delamination appeared to contribute somewhat to notched Izod impact strength. This was, however, not confirmed by the SENT fracture energy results.

The PC/ABS interface was investigated by testing of the weldline strength. Weldline strength of the blend was dramatically low compared to PC homopolymer containing a weldline. AN content in SAN did not appear to influence the weldline strength. Higher rubber content of the ABS increased weldline strength.

Acknowledgements

This work was sponsored by FOM, Fundamental Materials Research Program of the Netherlands. The authors wish to thank R.G. van Daele and B. Vastenhout, DOW Benelux, for the provision of all materials and TEM micrographs, and also Prof. dr.ir. L.C.E. Struik for stimulating discussions and support.

References

[1] Paul DR, Newman S, editors. Polymer blends, vols. I and II. New York: Academic Press, 1987.
[2] Paul DR, Barlow JW. J Macromol Sci, Rev Macromol Chem 1980;C18(1):109–68.
[3] Paul DR, Barlow JW, Keskkula H. In: Mark HF, Bikalos NF, Overberger CG, Menges G, editors. 2nd ed. Encyclopedia of polymer science and engineering, vol. 2. New York: Wiley, 1988. p. 399–461.
[4] Mamat A, Vu-Khanh T, Cigana P, Favis BD. J Polym Sci, Polym Phys 1997;35:2583–92.
[5] Lee MP, Hiltner A, Baer E. Polymer 1992;33(4):685–97.
[6] Guest MJ, Daly JH. Eur Polym J 1990;26(6):603–20.
[7] Willemse RC, Speijer A, Langeraar AE, Posthuma de Boer A. Polymer 1999;40:6645–50.
[8] Steenbrink AC, Gaymans RJ, Van der Giessen E. Polymat'94. 19–22 September. London, UK. p. 598–601.
[9] Keitz JD, Barlow JW, Paul DR. J Appl Polym Sci 1984;29:3131–45.
[10] Callaghan TA, Takakuwa K, Paul DR, Padwa AR. Polymer 1993;34(18):3796–808.
[11] Williams JG. Fracture mechanics of polymers. New York: Wiley, 1987.
[12] Havriliak Jr. S, Cruz Jr. CA, Slavin SE. Polym Engng Sci 1996;36(18):2327–44.
[13] Steenbrink AC, Janik H, Gaymans RJ. J Mater Sci 1997;32:5505–11.